

<b>ITC 4/53</b> Information Technology and Control Vol. 53 / No. 4/ 2024 pp. 1016-1027 DOI 10.5755/j01.itc.53.4.37133	<b>Instability Hazard Effect of Mined-out Areas Near the Mining Site by Fusion InSAR and PSO-BP Rock Mechanical Parameter Inversion</b>	
	Received 2024/04/30	Accepted after revision 2024/07/18
	<b>HOW TO CITE:</b> Yuan, L., Chen, D., Li, S., Wang, G., Li, Y., Peng, J., Qi, Z. (2024). Instability Hazard Effect of Mined-out Areas Near the Mining Site by Fusion InSAR and PSO-BP Rock Mechanical Parameter Inversion. <i>Information Technology and Control</i> , 53(4), 1016-1027. <a href="https://doi.org/10.5755/j01.itc.53.4.37133">https://doi.org/10.5755/j01.itc.53.4.37133</a>	

# Instability Hazard Effect of Mined-out Areas Near the Mining Site by Fusion InSAR and PSO-BP Rock Mechanical Parameter Inversion

**Liwei Yuan, Di Chen**

Faculty of Public Safety and Emergency Management, Kunming University of Science and Technology, Kunming, China

**Sumin Li**

Faculty of Land Resource Engineering, Kunming University of Science and Technology, Kunming, China

**Guolong Wang**

Faculty of Public Safety and Emergency Management, Kunming University of Science and Technology, Kunming, China

**Yanlin Li**

Yongshan Jinsha Lead-Zinc Mine Co., Ltd., Zhaotong, China

**Ji Peng, Zhuo Qi**

Faculty of Public Safety and Emergency Management, Kunming University of Science and Technology, Kunming, China

---

Corresponding author: [Lism@kust.edu.cn](mailto:Lism@kust.edu.cn)

---

Exploring the impact characteristics of near the mining activities on goaf and clarifying the disaster effects of instability in the mined-out area are critical research endeavors essential for effectively managing major risk hazards inherent to underground mining operations. This study integrates SBAS-InSAR and PSO-BP methodologies for inversely analyzing rock mechanical parameters in a lead-zinc deposit and applies the inversion results through the FLAC<sup>3D</sup> simulation method to the mining site adjacent to the null zone to study destabilizing disaster effects in the mined-out area under the influence of mining disturbance. The simulation aims to analyze the evolution process of surrounding rock destruction and instability in empty areas, identify the primary causes of disaster effects, develop a risk assessment and judgment model, and prevent accidents from occurring. The results of the study show that the integration of SBAS-InSAR and PSO-BP techniques for inverting rock mechanical parameters has yielded favorable outcomes in analyzing the destabilizing effect of the gob area near the mining site, and more accurately, it obtained the displacement and stress characteristics of the roof and pillars in the goaf under the mining disturbance as the mining near the empty area progresses. The simulation results demonstrate that influenced by mining disturbance, the maximum principal stress of the ore column in the void area significantly increases, primarily appearing as compressive stress. The distribution of the plastic zone indicates notably that the process of plastic deformation of the ore column leading to damage is primarily due to maximum shear stress. Evidently, the primary reason for the destabilization of the ore column is the concentration of stress resulting from mining disturbance, leading to compression and shear damage. FLAC<sup>3D</sup> simulation analysis has conclusively determined that pressure shear damage to the ore column resulting from undermining disturbance is the main cause of airspace destabilization in mining. The research methodology and analysis results provide vital theoretical support for the prevention and control measures against destabilization disasters in empty zones near mining sites, holding significant theoretical and practical value.

**KEYWORDS:** Numerical Simulation, Particle Swarm Optimization, Back-Propagation Neural Network, Computational Modeling.

---

## 1. Introduction

The destruction of the mining airspace is one of the hazardous sources often faced in the production process of underground mines, and the destabilization of the mining airspace has an obvious chain effect [10,14], the suddenness is difficult to predict and the seriousness of the hazards is the characteristics of its disasters and accidents, therefore, the use of fast and efficient methods and techniques of the stability of the mining airspace research, to explore the occurrence of null zone destabilization disaster mechanism and law appears to be more important and urgent, for the prevention and control of empty area destabilization disaster, to ensure the safe production of mine enterprises, is of great significance [7-8, 15]. Secondly, the increasing consumption of mineral resources, makes the mining environment gradually develop horizontally and vertically under the condition of limited mineable resources, resulting in a further increase in mining difficulty and more and more complicated surrounding rock stress in the mining area. At the same time, the peripheral rock of the mining area is very prone to accidents such as roof collapse,

water and sand gushing, and surface settlement under the action of rock creep and stress environment, and has an obvious chain relationship, and the accidents are diverse and very easy to be destabilized by the disturbance of the external environment. The stability of the mining area is affected by the complexity of many factors, and there is an urgent need to use scientific methods to analyze it in depth, to ensure its safety and stability. The mining of underground mineral resources is the fundamental cause of the movement of the surrounding rock and stress manifestation, using simulation technology to analyze the stability of the null zone, mainly to explore the mechanism of its internal stress and plasticity results. With the mining process, the stress distribution around the rock body will change, which will lead to the destruction of the rock layer, especially the mining of the near empty area, the rock movement law and disaster control is more complex [6], which is mainly the mining of the empty area by the adjacent area of the orebody in the mining process of disturbance, the coupling between the various influencing factors is a more complex

mechanism. Huang et al. [4, 6] tested and compared the settlement of the tunnel top and the ground surface as well as the settlement of the tunnel vault during the excavation process by studying the scaled model test of highway tunnel construction under a thin ore layer, and conducted stress analysis of the tunnel excavated near the mining void area, and the results showed that the horizontal coal seam has a great influence on the vertical pressure. Wang et al. [13] analyzed the movement law of the overlying strata with the mining of the ore layer under the mining void area, where the results showed that the collapse zone and fracture zone expand continuously to the surface with the mining. There are certain limitations in the rock mechanical parameters obtained from indoor tests for simulation analysis [3, 12]. The commonly used means for the study of the null zone are similar tests, theoretical analysis and simulation, and other technical means [1], the simulation technology has a lot of advantages compared with similar tests and theoretical analysis methods [6]. However, the accuracy of the simulation results is easily affected by the value of the rock mechanical parameters, and the accuracy and reasonableness of the rock mechanical parameters are extremely important, that is the basis for the numerical analysis of the stability of the goaf. Therefore, there are a large number of scholars combining the existing computer technology and other methods to invert the rock mechanical parameters, such as Cui et al. [3] proposed a composite model and use different models to invert different mechanical parameters, to get the proposed composite model for the surrounding rock mechanical parameters of the inversion of the results of the average error for the smaller, inversion trend and the actual displacement of highly similar. Liu et al. [9] developed a creep and shrinkage calculation model for elongated cylindrical rock salt caverns based on the complex variable theory, and determined the parameters of the creep model of rock salt Burgers under real conditions. Pan et al. [11] proposed a high-precision back-propagation neural network-particle swarm optimization (BP-PSO) algorithm inversion method to calibrate the micro-parameters of the cluster-particle logic concrete discrete element method model based on data similarity. Chen et al. [2] estimated the rock mechanics parameters based on semi-supervised support vector regression with data similarity. He et al. [5] proposed a method to introduce the deep convolution neural

network (DCNN) technique into the drilling process to continuously estimate rock field strength parameters, with the results validated in engineering.

For the current rock mechanical parameter inversion, the data samples are mainly based on one-sided data monitoring results, which is not only costly but also has a large subjectivity for the deployment of monitoring points, which has a certain impact on the accuracy of the final results. Therefore, the use of a reasonable and effective rock mechanical parameter inversion method is a problem worth exploring, based on the above deficiencies of the traditional rock mechanical parameter inversion method. In this study, a method is proposed to combine the advantages of the current InSAR monitoring technology, which can comprehensively monitor the ground surface in all weather conditions and has low cost, with the powerful nonlinear data generalization and mapping ability of the PSO-BP neural network. SBAS-InSAR (Small Baseline Subset Interferometric Synthetic Aperture Radar) combined with PSO-optimized BP neural network fusion technology is used to analyze the inversion of rock mechanical parameters of each rock layer in the study section of the research area, aiming to demonstrate the reliability and feasibility of SBAS-InSAR combined with PSO (Particle Swarm Optimization) optimized BP neural network in the inversion of rock mechanical parameters. At the same time, combined with the current near-empty zone mining has brought more challenges to the safety and stability of the mining zone, it is urgent to study the occurrence mechanism and law of the destabilization disaster of the mining zone under near-empty zone mining. Therefore, based on the inversion results of SBAS-INSAR and PSO-BP neural network algorithms, combined with FLAC<sup>3D</sup> numerical simulation technology, this article explores the instability disaster effect of empty zone under the influence of mining in near goaf, and analyzes the stress and displacement changes of surrounding rock under the influence of mining in near null area, aiming to explore the formation and development law of instability disaster in near mined-out area under the influence of mining.

This paper adopts SBAS-INSAR technology combined with PSO-BP neural network algorithm to invert the mechanical parameters of the overlying rock body in the mining airspace, which is convenient, fast and reliable to solve the parameter problem of rock

body mechanics in the process of analyzing the stability of the mining airspace using numerical simulation technology.

## 2. Background

### 2.1. Geological Conditions

The study area is located in a lead-zinc mine in Yongshan County, Yunnan Province. The strata are mainly divided into Quaternary, Cambrian Qiongzhusi Formation, Cambrian Meishucun Formation Dahai Section, Cambrian Meishucun Formation Zhongyicun Section, Cambrian Meishucun Formation Xiaoweitoushan Section, the Ediacaran Dengying Formation the first sub-section of the fifth section, the second sub-section of the fifth section.

The pre-mining orebody is mainly Phosphate Ore with an average dip angle of  $8^\circ$ ; the occurrence elevation of phosphate rock is between 1180 m and 1260 m and the thickness of the orebody is between 1.89 m and 9.9 m, with an average thickness of 5.91 m. The mining method is mainly room and pillar mining.

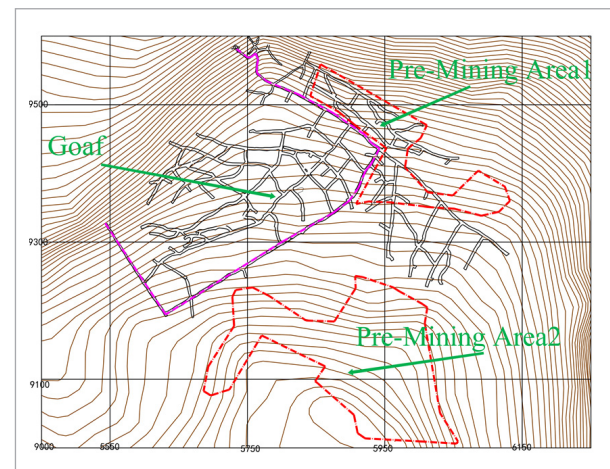
### 2.2. The Spatial Relationship Between the Empty Area and the Pre-mining Area

The pre-mining range 1 and the pre-mining range 2 are close to the goaf, and the pre-mining range 1 is connected with the empty zone in the northeast di-

rection, and the distance between the two is close. The pre-mining area 2 is located in the southeast direction of the mined-out area, and its main part has a certain distance from the goaf. The average elevation of the ore body in pre-mining scope 1 is around 1180m, and the vertical average thickness of the block section is 4.24m; the elevation of the ore body in pre-mining scope 2 is from 1216m to 1233m, and the vertical average thickness of the block section is 3.96m. The lowest point of the mining area has an elevation of 1180m, and the highest point has an elevation of 1240m. (Figure 1).

**Figure 1**

Spatial Position Relationship Between Goaf and Pre-mining Area



## 3. Inversion of Rock Mechanical Parameters Based on SBAS-InSAR and PSO-BP

This article selected four factors, including bulk, Poisson, cohesion, and friction, for inversion analysis. These factors are derived from the Quaternary Formation, the Cambrian Formation, and the Ediacaran Dengying Formation for a total of 12 factors. Therefore, the  $(L_{27}3^{12})$  orthogonal experimental table was selected in designing the orthogonal. In the selection of the parameter range, considering that the stratigraphic distribution of the same mining area is roughly the same, the rock body mechanical parameters of the neighboring mines can be used as a reference for determining the inversion parameter inter-

val. Combined with the distribution of the geological stratigraphic environment of the entire mining area, the parameter range of the mining section studied in this article is mainly determined with reference to the rock body parameters of other mining sections in the study area, the parameter range determined in this dissertation (Table 1).

Since this mining zone has been formed for three years, with time the mining zone will undergo creep deformation causing surface settlement, therefore, to obtain the surface deformation of the mining zone in the study area, the FLAC<sup>3D</sup> numerical simulation software will be used to analyze the creep of the mining zone. According to the Burgers-Mohr-Coulomb model selected for this paper, the roof, surrounding rock and mine house, and pillars of the mining void area were assigned to the Burgers intrinsic model, and the rest

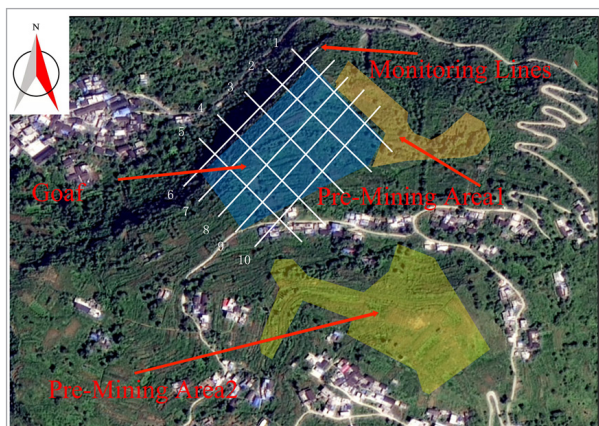
**Table 1**  
Selection Range of Rock Mechanics Parameters

Rock stratum	$Q^{ed1}$				$\epsilon_{1m}$				$Z_2dn^5$			
	Parameter / level	Bulk/GPa	Poisson	Cohesion/MPa	Friction/ $^\circ$	Bulk/GPa	Poisson	Cohesion/MPa	Friction/ $^\circ$	Bulk/GPa	Poisson	Cohesion/MPa
1	4.9	0.19	0.234	30.46	20.3	0.201	1.4	33.47	40.22	0.255	2.2	36.35
2	5.9	0.24	0.284	35.46	27.3	0.251	1.46	38.47	45.22	0.305	2.25	41.35
3	6.9	0.29	0.334	40.46	34.3	0.301	1.51	43.47	50.22	0.355	2.3	46.35

of the rock strata were assigned to the Mohr-Coulomb intrinsic model to conduct the creep analysis of the mining void area of the study area with a creep time of 3 years. In the selection of creep parameters, numerical simulation is used to determine their values by back-propagation in combination with the geological survey data of the mining area as well as references.

According to the above ontological model, FLAC<sup>3D</sup> was used for numerical analysis and then combined with the spatial location of the air-mining area, 10 monitoring lines were deployed in the area (Figure 2), and the SBAS-InSAR monitoring results and numerical simulation results were extracted from these 10 monitoring lines, and the numerical simulation results were used as the training set for the subsequent training of PSO-BP network algorithm for inversion of rock mechanics parameters, test and validation set data samples, and validation set data samples, according to the orthogonal test parameter combination data obtained from the surface settlement data

**Figure 2**  
Monitoring Line Position



using BP neural network to establish the mapping relationship between the rock body mechanical parameters and surface settlement, and finally through the SBAS-InSAR monitoring results as the input data of the trained network, and finally obtained a set of inversion results (Figures 3-4).

For each monitoring line, 30-35 data points were extracted, resulting in a total of 312 values for parameter

**Figure 3**  
The Error of InSAR vs FLAC<sup>3D</sup>

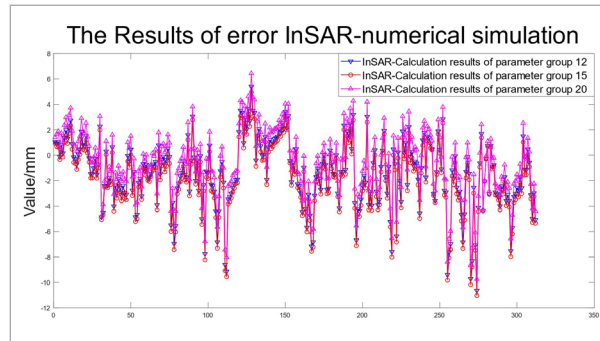
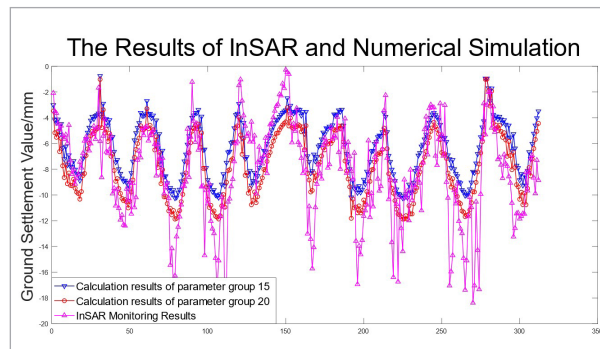


**Figure 4**  
The result of InSAR and FLAC<sup>3D</sup>



sets, and then the extracted displacement settlements were arranged according to the monitoring line numbers from 1 to 10 monitoring lines (Figure 4).

According to the numerical simulation results extracted in the previous section, 312 data in each group are used as the number of input samples in the training, testing, and validation sets of the neural network, so this article takes 312 data indicators as the number of input units of the neural network. The number of neurons of the implicit layer selected in this paper is 20; this article mainly analyzes the inversion of four rock mechanical parameters, such as the bulk, Poisson, cohesion, and friction, of three rock layers i.e. the quaternary, Cambrian, and the Ediacaran. The main purpose of this paper is to invert and analyze four rock mechanical parameters, and a total of 12 param-

eter values are needed to be output, so the number of output neurons selected in this article is 12.

In the implementation of the PSO-BP algorithm for the inversion of rock mechanics parameter, 27 sets of 312 columns of data totaling 8424 values were used as sample data. The first 75% is selected sequentially as the training set, 15% as the validation set, and the last 15% as the test set of the network. Meanwhile, to ensure the accuracy of the parameters obtained from the inversion and avoid the randomness and instability of the output of the network during the inversion process, in this article, when utilizing the PSO-BP network inversion method, 30 sets of inversion results are obtained by cycling 30 times, and the average value is selected as the final inversion result obtained by this method (Table 2).

Figure 5

Workflow diagram of research methodology

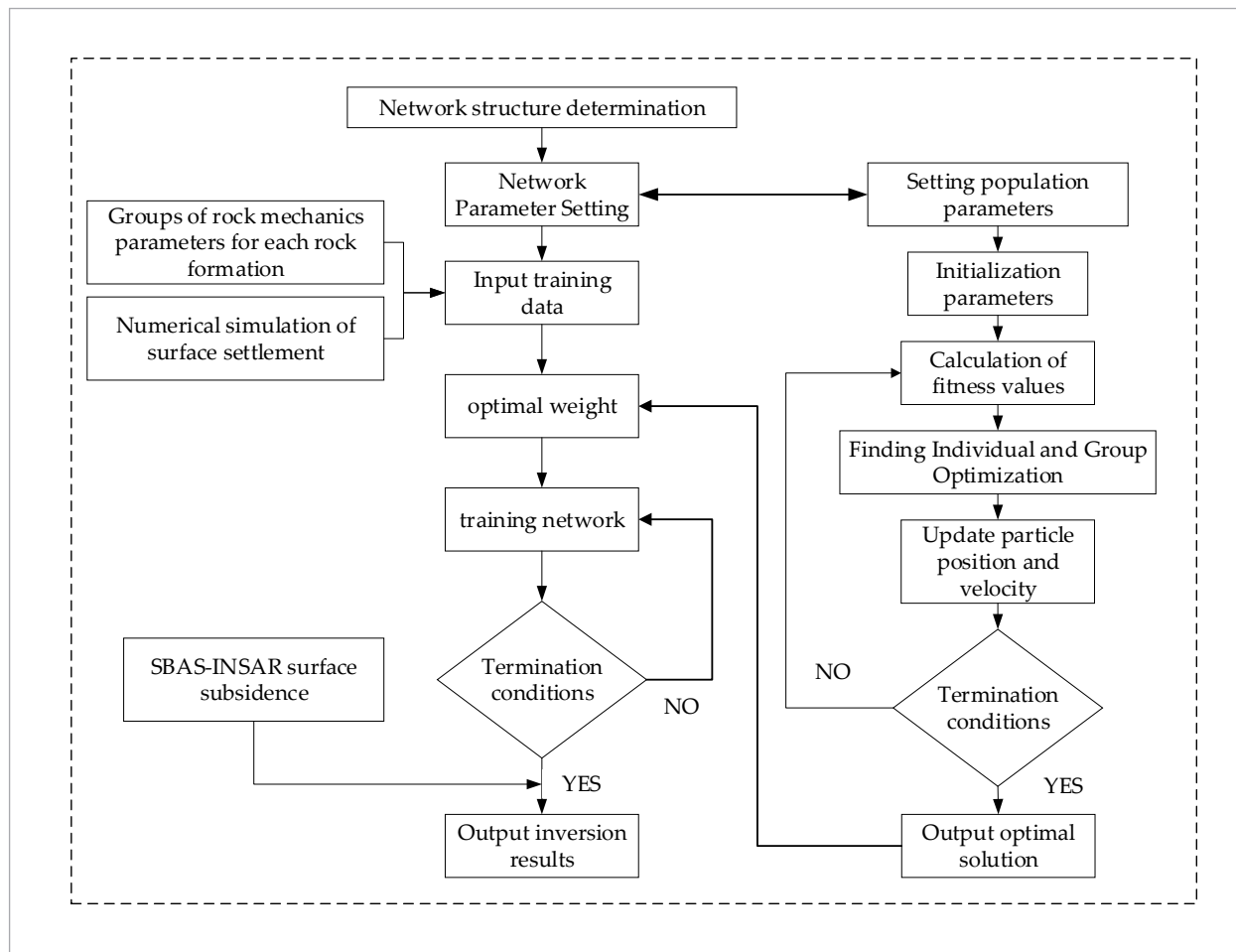


**Table 2**

The Final Inversion Results of Rock Mechanics Parameters of Each Rock Stratum in The Study Area

Rock stratum	$Q^{ed1}$				$\epsilon_{,m}$				$Z_2dn^5$			
Parameters	Bulk/ Pa	Poisson	Cohesion /Pa	Friction /°	Bulk/ Pa	Poisson	Cohesion /Pa	Friction /°	Bulk/ Pa	Poisson	Cohesion /Pa	Friction /°
Inversion results	6.60 E+09	0.232	2.80 E+05	34.023	2.45 E+10	0.272	1.47E+06	36.423	5.03 E+10	0.309	2.22 E+06	42.96

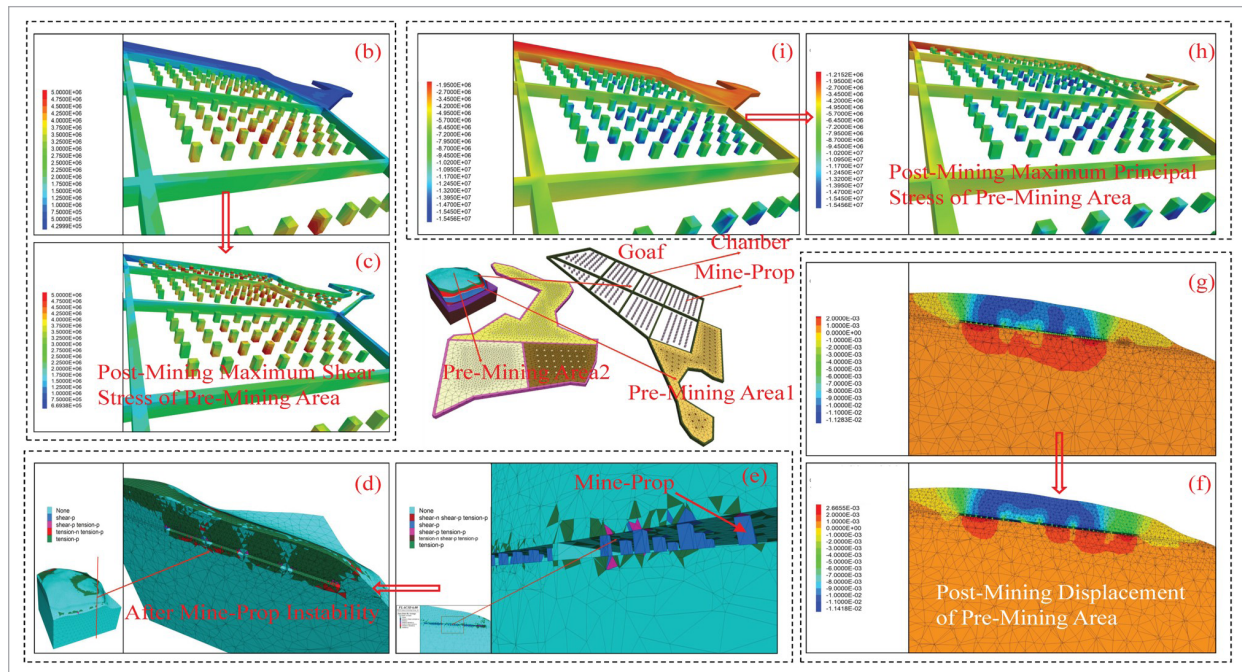
## 4. Simulation Analysis

Based on the inversion results of SBAS-InSAR and PSO-BP rock mechanical parameters, FLAC<sup>3D</sup> was used to study the destabilization hazard of the mining zone under the influence of mining in the adjacent void zone. A 750m×740m×420m model was established, and the mining pillar in the airspace area is 3m×3m, with a spacing of 9m. The pre-mining areas 1 and 2 which of the adjacent null area was mined through FLAC<sup>3D</sup>, to analyze the influence of the mining in the airspace area with the mining of the roof and pillar's displacement change, the change rule of the stress and the distribution of the plasticized zone. Mining of the pre-mining area began with creep calculations using the Burgers-Mohr-Coulomb model for the voided area, to simulate the stress distribution throughout the environment in which the voided area is located three years after its formation. To investigate the change in stress-strain as the excavation proceeds, the solution is performed in each stage. Stage 1: Creep solutions were performed on the mined-out areas for three years. Stage 2: Re-solve the initial stress after closing the creep, and excavate the pre-mining area 1 after stress equilibrium. Stage 3: Excavation of pre-mining area 2 after completion of excavation for pre-mining area 1. According to the preliminary Simulation results analysis, under the influence of mining disturbance in the adjacent mining airspace area mining column has the risk of instability, so to verify the stability of the mining airspace area in the case of column instability, numerical simulation of the mining airspace area under the conditions of column instability, and then analyze the simulation results of the maximum principal stress, the maximum shear stress and the distribution of the plastic zone, and the effect of the destabilizing disaster of the mining zone under the influence of mining in the adjacent hollow zone is further studied (Figure 6) With the excavation of the adjacent pre-mining area of the

void zone, the displacement of the roof plate of the void zone increased (compare in Figure 6(f)-(g)), indicating that by the influence of the mining of the adjacent pre-mining area of the void zone 1 and pre-mining area 2, the stress equilibrium formed in the void zone after a long time was broken, which disturbed the stress state of the original rock layer and led to a further increase in the displacement value of the roof plate of the void zone and the surrounding rock. The maximum principal stress of the pillar increases mainly in compressive stress, and the largest change in principal stress is mainly near the pre-mining area 1 of the mining pillar, the mining pillar farther from the pre-mining area 1 of the mining pillar part of the pillar maximum principal stress has changed to a certain extent, but the degree of change is not very obvious compared with the closer distance down the pillar (compare in Figure 6(i)-(h)). Secondly, the minimum principal stress and maximum shear stress of the roof plate and ore pillar in the mining area were analyzed (compare in Figure 6(b)-(c)). Similarly, the stress variation of the ore pillar and roof plate in the part closer to the pre-mining area 1 is more obvious, in which the maximum shear stress variation of the ore pillar is around 0.5 Mpa. For the analysis of the displacement and stress change of the roof plate, it was obtained that the displacement change of the roof plate was more obvious in the place closer to the pre-mining area 1; however, the stress did not show obvious tensile stress phenomenon, and it was mainly affected by the role of the overlying rock pressure and the support of the mine pillar in the mining hollow area, which showed that the roof plate in the mining hollow area was mainly controlled by the pressure.

According to the analysis of simulation results, when the mining hollow area column damage destabilization after mining hollow area overlying rock layer appeared a large area of plastic zone, most of which has been through the surface, and the main plastic zone is caused by tensile stress damage (Figure 6(d)-(e)).

**Figure 6**  
Numerical Simulation Results of FLAC<sup>3D</sup>



## 5. Discussion

1 To verify the rationality and accuracy of the inversion results. The correlation coefficient is used to analyze the correlation between the SBAS-InSAR monitoring results and the simulation results, and the correlation between the two sets of data is determined by calculating the Pearson correlation coefficient of the two sets of data (Figure 7(e)). The results show that there is a good correlation between the inversion sample data. The network performance and calculated data results are discussed as a way to analyze the reliability of the results (Figure 7(f)). During the training process of the inversion network, the fit of the training set, validation set, test set, and overall data is superior, with a fit of 99%, which can meet the requirements when inverting rock mechanical parameters. For the calculation results, the error analysis is mainly used to discuss the reliability, according to the RMSE plot analysis (Figure 7(a)-(d)), Which are fluctuating within a certain range, indicating that the inversion results are still relatively stable and reliable. The RMSE all fluctuates with a certain period, which precisely indicates that the change

of regression accuracy during the network training process when the network is being trained will have a certain impact on the stability of the inversion results.

In this article, although the FLAC<sup>3D</sup> numerical simulation process is used to simulate the displacement and strain under the influence of mining in the adjacent air zone, and certain conclusions have been obtained. However, for the more microscopic rock damage mechanism has not yet been explored, the use of FLAC3D numerical calculations, only simulated the general macro-basic laws, for the deeper causal mechanism of the investigation needs to be strengthened.

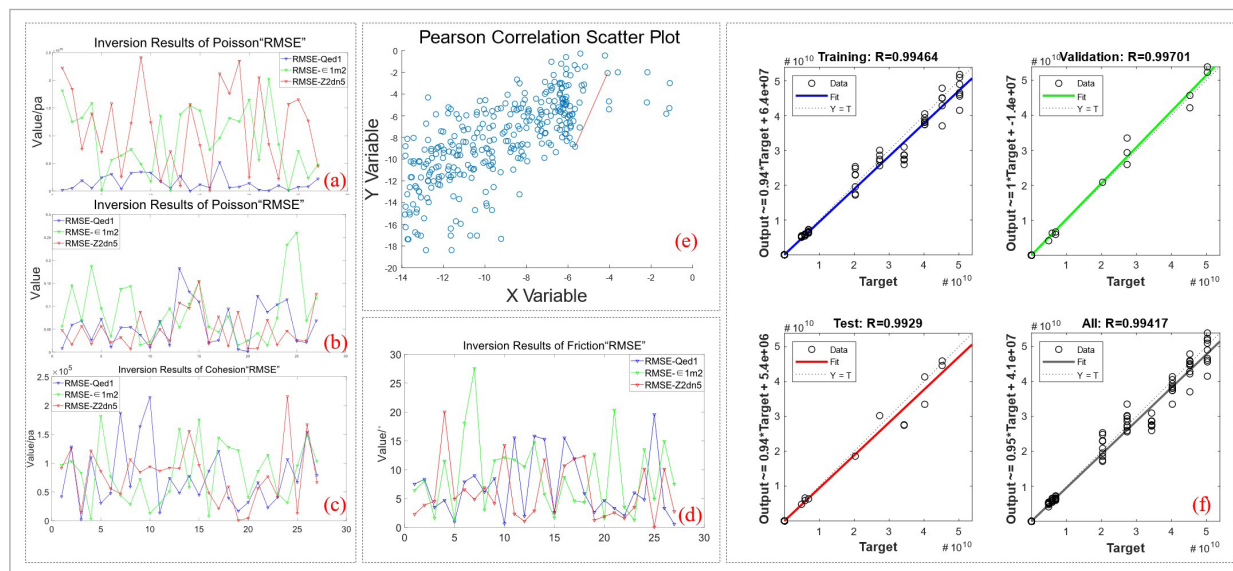
2 According to the discussion on the simulation of displacement stress and plastic zone distribution before and after mining in the pre-mining area, it is obtained that the displacement of the roof plate and pillars in the mining hollow area changed significantly, in which the maximum displacement value of the roof plate in the Z direction increased from 11.283 mm to 11.418 mm, and the maximum displacement value of the Y direction increased from 7.5713 mm to 7.8245 mm; and the deformation of the

pillar near the pre-mining area 1 was larger than that of the other pillars. Secondly, several aspects such as maximum principal stress, minimum principal stress, maximum shear force, and minimum shear force of the ore column in the mining hollow area are analyzed and discussed, and according to the simulation results, it is obtained that with the mining of the pre-mining area, the maximum principal stress, minimum principal stress, maximum shear force and minimum shear force of the ore column change significantly. Finally, the analysis of the mine pillar and the plastic zone of the roof plate in the hollow area after mining in the pre-mining area shows that the plastic zone of the mine pillar is affected by the

compression and shear damage and the plastic zone of the mine pillar is close to the pre-mining area 1 part of the mine pillar has obvious plastic zone penetration, and the plastic zone of the roof plate is mainly concentrated in the area around the mine pillar and is mainly for the tensile damage and shear damage. It can be seen that the roof is less affected by mining in the pre-mining area, so the risk of roof instability is less than that of the pillars. To verify whether the destabilization of the mining pillar in the airspace area can lead to the overall destabilization of the goaf, the stability change of the airspace area was simulated after the loss of the bearing capacity of the pillar.

Figure 7

Analysis of Inversion Result Data



## 6. Conclusion

- 1 The inversion results of rock body mechanical parameters carried out by SBAS-InSAR and PSO-BP technology were used to analyze the destabilizing disaster effect of the mining area under the influence of mining disturbance in the adjacent airspace area achieved good results. In the PSO-BP network training of the regression fit goodness of R were 0.994, 0.997, 0.992, the fitting effect can meet the requirements of inversion, the sample data and results are analyzed. It shows that the inversion effect of the mechanical parameters of the rock body in the mining hollow area using this method is reliable.
- 2 Analyze the destabilization disaster of the hollow zone under the influence of mining disturbance in the adjacent hollow zone, and the results show that the pressure-shear damage of the ore column under the mining disturbance is the main reason for the destabilization of the hollow zone. Under the influence of mining disturbance in the near mining area, the displacement of mine pillar and roof plate in the hollow zone changes obviously with the influence of mining in the pre-mining area 1 and pre-mining area 2, and the main influence range is the part close to the pre-mining area

1. According to the analysis results, the main risk of destabilization of the hollow zone under the influence of mining disturbance near the hollow zone may be caused by the destabilization of the ore column.

## Acknowledgment

The authors gratefully acknowledge the financial support for this project from the National Natu-

ral Science Foundation of China Research on Slope Instability and Surface Deformation Behavior Patterns in High Altitude and Cold Mining Areas (Grant No.53264020), At the same time, The authors gratefully acknowledge the Yongshan Jinsha Lead-zinc Mine Co., Ltd. to provide research background. They also acknowledge the contributions of the authors of the references cited and the valuable feedback received from reviewers and mentors.

## References

- Chai, J., Ouyang, Y., Liu, J., Zhang, D., Du, W., Lei, W. Experimental Study on a New Method to Forecasting Goaf Pressure Based Key Strata Deformation Detected using Optic Fiber Sensors. *Optical Fiber Technology*, 2021, 67, 102706-102706. <https://doi.org/10.1016/j.yofte.2021.102706>
- Chen, X., Cao, W., Gan, C., Ohyama, Y., She, J., Wu, M. Semi-Supervised Support Vector Regression Based on Data Similarity and Its Application to rock-Mechanics Parameters Estimation. *Engineering Applications of Artificial Intelligence*, 2021, 104, 104317. <https://doi.org/10.1016/j.engappai.2021.104317>
- Cui, J., Wu, S., Cheng, H., Kui, G., Zhang, H., Hu, M., He, P. Composite Interpretability Optimization Ensemble Learning Inversion Surrounding Rock Mechanical Parameters and Support Optimization in Soft Rock Tunnels. *Computers and Geotechnics*, 2024, 165, 105877-105877. <https://doi.org/10.1016/j.compgeo.2023.105877>
- Fang, Y., Xu, C., Cui, G., Kenneally, B. Scale Model Test of Highway Tunnel Construction Underlying Mined-Out Thin Coal Seam. *Tunnelling and Underground Space Technology*, 2016, 56, 105-116. <https://doi.org/10.1016/j.tust.2016.03.007>
- He, M., Zhang, Z., Ren, J., Huan, J., Li, G., Chen, Y., Li, N. Deep Convolutional Neural Network for Fast Determination of the Rock Strength Parameters Using Drilling Data. *International Journal of Rock Mechanics and Mining Sciences*, 2019, 123, 104084. <https://doi.org/10.1016/j.ijrmms.2019.104084>
- Huang, F., Shi, X., Wu, C., Dong, G., Liu, X., Zheng, A. Stability Analysis of Tunnel under Coal Seam Goaf: Numerical and Physical Modeling. *Underground Space*, 2023, 11, 246-261. <https://doi.org/10.1016/j.undsp.2022.12.006>
- Ke, L., Wu, M., Ye, Y., Hu, N., Meng, Y. Stability Risk Early Warning for Mine Goaf: Based on D-RES and Asymmetric Fuzzy Connection Cloud Model. *Journal of Computational Science*, 2024, 78, 102279-102279. <https://doi.org/10.1016/j.jocs.2024.102279>
- Li, M., Li, K., Liu, Y., Wu, S., Qin, Q., Yue, R. Goaf Risk Prediction Based on IAQA-SVM and Numerical Simulation: A Case Study. *Underground Space*, 2024, 15, 153-175. <https://doi.org/10.1016/j.undsp.2023.07.003>
- Liu, Y., Li, Y., Shi, X., Ma, H., Zhao, K., Dong, Z., Hou, B., Shangguan, S. Creep Monitoring and Parameters Inversion Methods for Rock Salt in Extremely Deep Formation. *Geoenergy Science and Engineering*, 2023, 229, 212092. <https://doi.org/10.1016/j.geoen.2023.212092>
- Ma, H., Wang, J., Wang, Y. Study on Mechanics and Domino Effect of Large-Scale Goaf Cave-in. *Safety Science*, 2012, 50(4), 689-694. <https://doi.org/10.1016/j.ssci.2011.08.050>
- Pan, X., Niu, Y., Zhao, Y., Huang, P., Wu, Y. Parameter Calibration Method of Clustered-Particle Logic Concrete DEM Model Using BP Neural Network-Particle Swarm Optimisation Algorithm (BP-PSO) Inversion Method. *Engineering Fracture Mechanics*, 2023, 292, 109659-109659. <https://doi.org/10.1016/j.engfracmech.2023.109659>
- Sun, W., Chen, L., Guo, W., Wu, S., Meng, S. Modeling of Spalling Failure of In-Situ Rock Mass for Quantification of the Source Mechanics with Flat-Joint Model and Moment Tensor. *Computers and Geotechnics*, 2024, 169, 106261-106261. <https://doi.org/10.1016/j.compgeo.2024.106261>
- Wang, F., Zhang, C., Zhang, X., Song, Q. Overlying Strata Movement Rules and Safety Mining Technology for the Shallow Depth Seam Proximity Beneath a Room Mining Goaf. *International Journal of Mining Science and Technology*, 2015, 25(1), 139-143. <https://doi.org/10.1016/j.ijmst.2014.12.007>
- Wang, J., Yang, L., Li, F., Wang, C. Force Chains in Top Coal Caving Mining. *International Journal of Rock Mechanics and Mining Sciences*, 2020, 127, 104218-104218. <https://doi.org/10.1016/j.ijrmms.2020.104218>
- Zhang, B., Hu, S., Li, M. Comparative Study of Multiple Machine Learning Algorithms for Risk Level Prediction in Goaf. *Heliyon*, 2023, 9(8), e19092-e19092. <https://doi.org/10.1016/j.heliyon.2023.e19092>

## Appendice: Pseudocode of the Algorithm

---

```

1: // Clear workspace, and close all figures.
2: // Read data from Excel files:
3: // Prepare training and testing data:
   input_train = data1(:, 1:n)
   output_train = data2(:, 1:n)
   input_test = data1(:, n+1:end)
   output_test = data2(:, n+1:end)
4: // Normalize the input and output training data:
   normalized_input_train, input_norm_params =
   normalize(input_train, 0, 1)
   normalized_output_train, output_norm_params
   = normalize(output_train, 0, 1)
5: // Define the number of nodes:
   input_nodes = number_of_rows(normalized_in-
   put_train)
   output_nodes = number_of_rows(normalized_
   output_train)
6: // Construct the neural network:
   net = create_network(normalized_input_train,
   normalized_output_train, hidden_nodes, 'tan-
   sig', 'purelin', 'trainlm')
   net.train_params.epochs = 1000
   net.train_params.learning_rate = 0.1
   net.train_params.goal = 0.00001
7: // Initialize PSO algorithm parameters:
8: // Calculate the total number of nodes:
   total_nodes = input_nodes * hidden_nodes + hid-
   den_nodes + hidden_nodes * output_nodes + out-
   put_nodes
8: // Initialize particles and velocities:
   for each particle in population:
   particle = 5 * random_values(total_nodes)
   velocity = random_values(total_nodes)
   fitness = calculate_fitness(particle, input_nodes,
   hidden_nodes, output_nodes, net, normalized_
   input_train, normalized_output_train)
9: // Determine initial global and individual bests:
   best_fitness, best_index = minimum(fitness)
   global_best = particles[best_index]
   individual_bests = particles
   individual_best_fitnesses = fitness
   global_best_fitness = best_fitness
10: // Perform PSO optimization:
   for generation in 1 to max_generations:
   for each particle in population:
   w = w_max - (w_max - w_min) * generation /
   max_generations
   velocity = update_velocity(velocity, c1, c2, in-
   dividual_best, global_best, particle, w)
   particle = update_position(particle, velocity,
   pop_max, pop_min)
   if random_value > 0.9:
   randomize_particle(particle)
   fitness = calculate_fitness(particle, input_
   nodes, hidden_nodes, output_nodes, net,
   normalized_input_train, normalized_out-
   put_train)
   if fitness < individual_best_fitness:
   individual_best = particle
   individual_best_fitness = fitness
   if fitness < global_best_fitness:
   global_best = particle
   global_best_fitness = fitness
   record_best_fitness(generation, global_
   best_fitness)
   x = global_best
11: // Assign optimized weights and biases to the neu-
   ral network:
   w1 = extract_weights(x, 1, input_nodes * hidden_
   nodes)
   B1 = extract_weights(x, input_nodes * hidden_
   nodes + 1, hidden_nodes)

```

---

---

```
w2 = extract_weights(x, input_nodes * hidden_
nodes + hidden_nodes + 1, hidden_nodes * out-
put_nodes)
```

```
B2 = extract_weights(x, input_nodes * hidden_
nodes + hidden_nodes + hidden_nodes * output_
nodes + 1, output_nodes)
```

```
set_network_weights(net, w1, B1, w2, B2)
```

---

```
12: // Train the neural network:
```

```
net, training_performance = train_network(net,
normalized_input_train, normalized_output_train)
```

---

---

```
13: // Perform prediction using the trained network:
```

```
normalized_input_forecast = apply_normaliza-
tion(data3, input_norm_params)
```

```
output_forecast = simulate_network(net, nor-
malized_input_forecast)
```

```
final_output = reverse_normalization(output_
forecast, output_norm_params)
```

```
End
```

---



This article is an Open Access article distributed under the terms and conditions of the Creative Commons Attribution 4.0 (CC BY 4.0) License (<http://creativecommons.org/licenses/by/4.0/>).